CONF-761107--22

HYDRODYNAMIC INSTABILITY INDUCED LIQUID-SOLID CONTACTS IN FILM BOILING

Shi-chune Yao and Robert E. Henry

ASME Meeting
December 5, 1976
New York

ARGONNE NATIONAL LABORATORY, ARGONNE, ILLINOIS

operated under contract W-31-109-Eng-38 for the
U. S. ENERGY RESEARCH AND DEVELOPMENT ADMINISTRATION

ABSTRACT

The film boiling liquid-solid contacts of saturated ethanol and water to horizontal flat gold plated copper are examined by using electric conductance probe. It is observed that the liquid-solid contacts occur over a wide temperature range and, generally, induced by hydrodynamic instabilities. The area of contact decreases exponentially with interface temperature and is liquid depth dependent. The averaged duration of contacts is strongly influenced by the dominant nucleation process, and thus, depends on the interface temperature and the wettability of the solid during the contact. The frequency of major contacts is about 1.5 times the bubble detaching frequency. It is found that the liquid-solid contacts may account for a large percentage of the film boiling heat transfer near the low temperature end of film boiling and decreases as the interface temperature increases.

NOMENCLATURE

a	fraction of solid area where contacts occur
A	area of contact
A_p	effective area of probes on resistance evaluation
C	heat capacitance
erf	error function
f	frequency
f(θ)	a function of contact angle
g	gravity
h	Plank constant
J^p	embryo formation frequency per unit volume
k	thermal conductivity
K	Boltzman constant
L	normal distance between probe and dish
n	ratio of vapor film thickness to L
n	molecular density
P	pressure
q	heat flux
Q	heat
R	electric resistance
t	time
T	temperature
T^*	nondimensional temperature defined as $(T - T_b)/(T_c - T_b)$
v	contact signal voltage
V	battery voltage
W	work function
x	distance from interface

Greek Symbols

α	thermal diffusivity
β	contact angle measured through liquid
Δ	differential notation
λ_D	most dangerous wavelength, Eq. (1)
ρ	density or electric resistivity
σ	surface tension of liquid to vapor

Subscripts

b	boiling or bubble
c	thermodynamic critical state or contact
fb	film boiling
i	interface
l	liquid
min	at minimum heat flux in film boiling
s	solid
v	vapor

INTRODUCTION

An understanding of liquid-solid contact behavior and the associated heat transfer in film boiling is of importance in the interpretation of quenching heat flux energy transfer results as well as emergency core cooling data for water reactors.

When the liquid is subcooled, the vapor generation in film boiling is suppressed. The liquid-solid contact, at this stable film boiling, was observed by Bradfield [1], and it was found that the liquid subcooling and surface roughness play important roles in the occurrence of contacts. Sadasivan and Lienhard [2] calculated the periodic quenching in transition boiling regime using transition boiling heat transfer data, but the results cannot be extrapolated to the film boiling region. The instability induced contacts in liquid-liquid film boiling noticed by Henry et al. [3], in experiments for lighter liquid on mercury. Recently, Swanson et al. [4] measured the solid surface temperature variations in film boiling and confirmed the contact hypothesis. However, through their indirect method, they were not able to arrive at a quantitative description of the contact behavior. In a recent paper by Bjorge et al. [5], the direct contact heat transfer of drops to a wall was included in a model of dispersed flow heat transfer. The overall heat transfer data were correlated but since the contact heat transfer data are not available, the proposed model could not be confirmed.

In the present experiment, the hydrodynamic instability induced liquid-solid contacts of saturated ethanol and water are examined by electric conductance probes. The objective of this paper is to investigate:

a. The various nucleation processes near the contact interface.

b. The liquid-solid contact behavior in film boiling, e.g., the area, duration, and frequency of contacts.

c. The contribution of contact heat transfer to the overall film boiling heat transfer.

EXPERIMENTAL APPARATUS AND PROCEDURES

These film boiling experiments were conducted on the copper plate illustrated in Fig. 1. In order to prevent excessive oxidation of the copper at high temperatures needed for this boiling regime, the upper polished surface of the dish was plated with a 15 μ soft gold layer, which was 99.9% pure. The similar thermal properties of the gold and copper assure that the interface thermal behavior will not be significantly affected during liquid-solid contacts. Cobalt and other impurities in commercially available hard gold were observed to oxidize at the elevated temperatures which necessitated the use of the soft gold plating. In addition, since physical and chemical cleanliness were essential, the experiments were performed in an argon gas glove box, which minimized airborne particulate impurities and also minimized the oxidation potential for any remaining impurities within the soft gold. As a final precaution, only reagent grade ethanol and triple distilled (quartz still) water were used as boiling liquids.

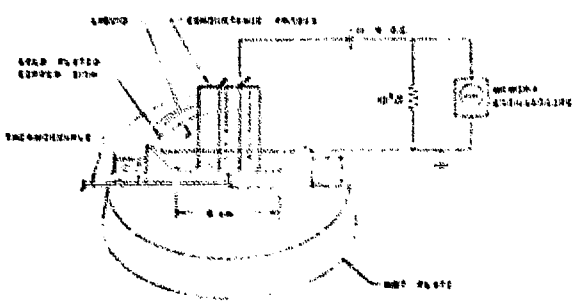

Fig. 1. Schematic of experimental set-up.

The copper plate was heated from below by 660 W heater and the wall temperature was measured by a grounded sheath thermocouple inserted to within 0.8 mm below the surface. The liquid-solid contacts during film boiling were detected by measuring the electrical conductance between the boiling liquid globule and the solid dish. As illustrated in Fig. 1, the probes were inserted into the liquid to within 1.5 mm of the solid surface, and the voltage difference across the resistor was recorded by a memory oscilloscope. The relationship between the film boiling behavior and the voltage signals was examined by high-speed movies which simultaneously recorded the liquid behavior and the oscilloscope trace.

In conducting these experiments, the dish was first heated to the desired temperature and then the boiling liquid was poured onto the surface. In this experimental configuration, the oscillating liquid boundary and the solid wall may provide a varying electrical capacitance. In order to ascertain the importance of such a varying capacitance on the voltage signal, tests were performed with different electric conductivities by adding minute amounts of KNO_3 to the water. The additive should remain in the water as opposed to the vapor film. It was observed that the voltage output was proportional to the liquid electric conductivity and the normalized signal shapes remained the same, which indicates that the contribution of varying capacitance was insignificant in the observed signals which represent physical liquid-solid contacts.

EXPERIMENTAL RESULTS

Effects of Hydrodynamic Instability

The film boiling heat transfer process from a horizontal flat plate has been studied experimentally and analytically in terms of the Taylor instability phenomenon. In this mechanism, the vapor is removed from the heated surface through vapor domes which grow into large bubbles, depart, and allow the liquid to return to the surface with alternate vapor domes being initiated at the anti-node between the original bubbles. The distance between these departing bubbles near the minimum film boiling point was proposed by Berenson (6) to be equal to the most dangerous wave length dictated by the Taylor instability.

$$\lambda_D = 2\pi \left(\frac{3\sigma}{g(\rho_\ell - \rho_v)} \right)^{1/2} . \qquad (1)$$

This spacing was demonstrated in the experiments of Hosler and Westwater (7) to be a good average representation of the vapor departure conditions. The high speed movies taken in the present water experiment show that the averaged observed spacing is 2.97 cm which is in good agreement with the predicted value of 2.72 cm by Eq. (1). The number of departure sites/cm² appear to be somewhat lower than the prediction by assuming a square pattern of bubbles and the most dangerous wave length, but this is attributable to the edge effect of the finite size of liquid layer that could be used on this test piece. Since the most dangerous wave length for ethanol is less than that for water, the edge effect is less significant.

In present experiments of saturated liquids, the major liquid/solid contacts occur when the bubble departs from a given node and the liquid retracts back towards the surface. In these experiments, only liquid globules which were much larger than the most dangerous wave length were utilized so that the presence of the Taylor instability phenomena, and the accompanying mechanical disturbances were definitely present. These large globules prevent the onset of metastable effects as observed by Baumeister and Henrichs (8) for small drops.

In this study, several types of liquid-solid contacts were observed within the film boiling regime, and these are characterized in Fig. 2. The first type of contact was a shallow bubble which did not detach from the liquid layer, but moved towards the periphery of the liquid layer and finally escaped when it reached the outer regions. This type of contact produced a continual traveling contact along the bottom interface. This type of contact records a small magnitude but a long duration contact on the oscilloscope. When the diameter of the liquid layer is slightly increased, single bubbles appear and detach at the center of the layer with relatively low frequency. As illustrated in Fig. 2(b), whenever a bubble detaches, the liquid layer collapses onto the solid and distinct liquid-solid contacts are observed. These may be composed of a group of contacts with the major ones being more

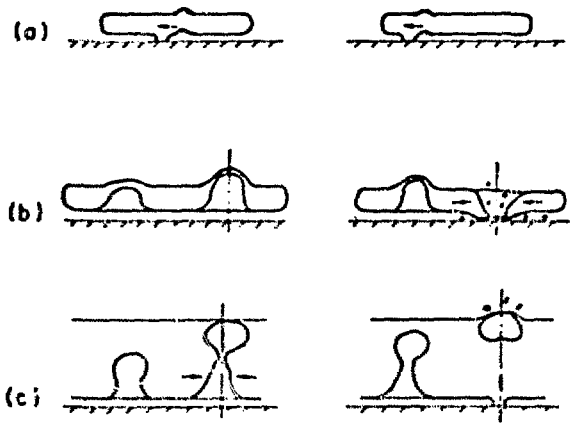

Fig. 2. Schematics of three types of liquid-solid contact in horizontal plate film boiling.

prominent and the smaller ones resulting in small fragmented drops which then leave the liquid layer and sputter around the hot surface. As the diameter of the liquid layer increased, more bubbles appear and the contacts are observed with higher frequencies. When the depth of the pool is further increased, as in Fig. 2(c), bubbles are observed to detach and rise vertically within the liquid with a liquid jet impinging upon the solid at the point of bubble departure. Some additional minor contacts are also observed at the periphery of the liquid pool and these appear to be induced by surface ripples.

The bubble detach frequencies and the liquid-solid contact frequencies were observed in the experiment through the movie and oscilloscope results. Both the frequencies are found to be linear proportional to the difference between the solid temperature and the liquid saturation temperature. As is shown in Fig. 3, the frequencies of major liquid-solid contacts is about 1.5 times the bubble frequencies.

$$f_c = 1.5\, f_b \,. \tag{2}$$

It was reported that at much higher temperatures the bubble generation rate is so high that the detaching of bubbles may not induce anti-nodes (9). As a result, the relationship between the two frequencies should not be extended without verification to temperatures far beyond the range of present experiment.

Effects of Contact Interface Temperature

There are several temperatures used to characterize the physical behavior in the film boiling process. The two most commonly used temperatures are the fluid saturation temperature and the wall temperature which represent a value measured by a thermocouple imbedded within the solid wall. Another temperature, that discussed by Henry (10), is the interface temperature upon contact between the liquid and the wall, and this can be evaluated from the parabolic heat conduction equation with constant thermal-physical properties and uniform initial temperatures within the wall and the liquid (11) by

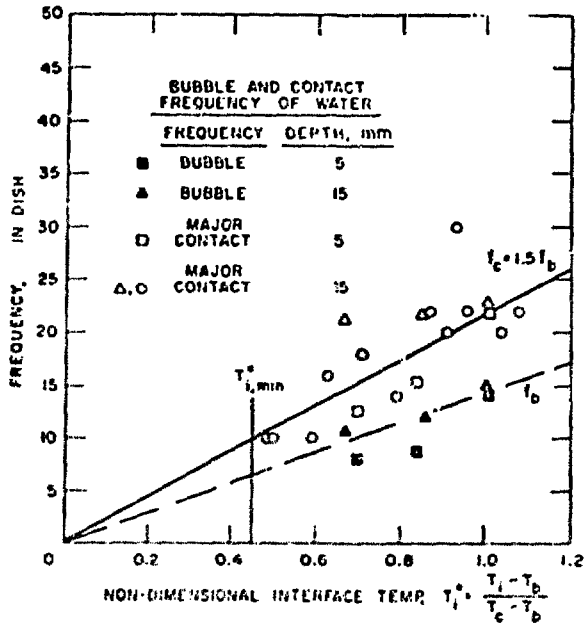

Fig. 3. Film boiling bubble frequency and liquid-solid contact frequency of water.

$$T_i = \frac{T_s + T_b\sqrt{k_l\rho_l C_{p_l}/k_s\rho_s C_{p_s}}}{1 + \sqrt{k_l\rho_l C_{p_l}/k_s\rho_s C_{p_s}}} \,. \tag{3}$$

This value represents the instantaneous contact temperature as long as the time scale of interest is greater than 10^{-12} s. This interface temperature can be expressed in a nondimensional form in terms of the fluid saturation temperature and the thermodynamic critical temperature as

$$T^*_i = \frac{T_i - T_b}{T_c - T_b} \,. \tag{4}$$

Two other temperatures of interest in the interpretation of these experiments are the thermodynamic critical temperature and the spontaneous nucleation temperature. Spontaneous nucleation results from density fluctuations within the boiling liquid and can be calculated from classical nucleation theory. The frequency of formation of critical size vapor cavities is represented by (12):

$$J = n\left(\frac{KT}{h_p}\right)\exp\,(-W/KT), \tag{5}$$

where W is the work required to form a critical size spherical vapor bubble and can be approximated for low pressures by

$$W = 16\pi\sigma^3 f(\theta)/(3P_v^2), \tag{6}$$

where the function $f(\theta)$ is a function of the contact angle through the liquid and can be evaluated from

$$f(\theta) = (1/4)(1 + \cos\theta)^2 (2 - \cos\theta). \quad (7)$$

When the contact angle equals zero, the critical size cavities are formed solely within the bulk of the boiling liquid and this form of spontaneous nucleation is termed homogeneous nucleation. For other values of contact angle, the nucleation is still spontaneous, but the critical size vapor cavities are formed at the interface between the boiling liquid and the heated wall and this is termed heterogeneous nucleation. The spontaneous nucleation densities of ethanol and water are shown in Fig. 4 with different values of contact

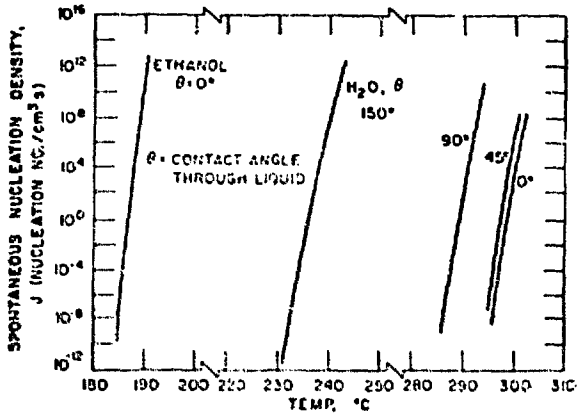

Fig. 4. Spontaneous nucleation density of ethanol and water.

angles. The nondimensionalized homogeneous nucleation temperature of ethanol and water is 0.69 and 0.74 for nucleation densities equal to 10^{10} per cm^3 per s. A third type of nucleation which must be contented with in liquid-solid boiling systems is a nucleation from preferred sites with a pre-existing liquid-vapor interface. It is this kind of nucleation which governs the normal nucleate boiling regime and certain portions of the film boiling regime. However, as the interface temperatures upon contact become extremely large, the homogeneous nucleation rate increases by orders of magnitude and becomes a predominant mechanism for the formation of vapor embryos. If this frequency range and the corresponding period far exceeds the response time of normal surface cavities, then the film boiling behavior may be entirely dependent upon the spontaneous nucleation characteristics of the system.

In the experiment the liquid-solid contacts are observed as voltage signals which indicate the corresponding electric resistance across the probes and the solid disk in a contact. During a contact, the electrical path in the liquid is composed of two regions. As illustrated in Fig. 2, one is a shallow liquid cylinder making contact with the solid with a height equals the vapor film thickness and the other region is the extended liquid layer where the probes are inserted in. The electric resistance of each of the two regions can be approximated by the resistance between two parallel discs. For the parallel disc geometry, the resistance is inversely proportional to the square root of the product of the disc areas. As a result, the voltage signal, v, and the area of contact can be related as

$$\frac{v}{V} = \frac{R}{R + \rho L \left(\frac{m}{A} + \frac{m}{\sqrt{A\, A_p}} \right)}, \quad (8)$$

where mL is the vapor film thickness which can be estimated from (6), R is the resistance across which the contact signals are measured, and A_p is the effective disc area of the probes which was evaluated through calibrations. Additionally, the contact area can be presented as a fraction of the area of one bubble site which equals λ_D^2 for square pattern bubble distribution. Therefore, the fraction of area where a contact covers is

$$a = \frac{A}{\lambda_D^2}. \quad (9)$$

Based upon these arguments, Fig. 5 is established to evaluate the contact area fractions from the contact voltage signals.

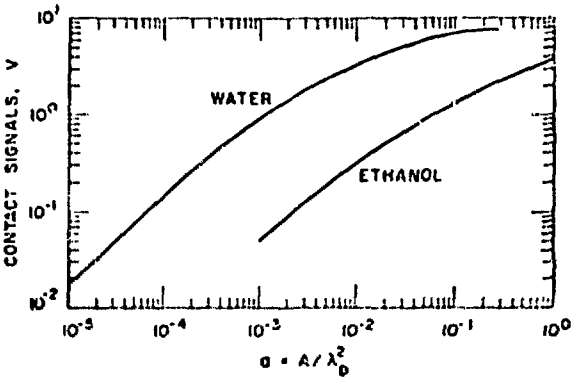

Fig. 5. The relation between normalized contact area to the voltage reading of the contact signals.

It was found that the liquid-solid contacts occur over wide temperature range. Some typical contact signals of ethanol and water on gold plated copper are shown in Figs. 6 and 7, respectively, with voltage signals as the ordinate and time as abscissa. Figures 6(d) to 6(g) and 7(b) to 7(f) contain superimposed contact signals. The contact area fraction of ethanol and water are presented in Figs. 8 and 9, respectively, as a function of the nondimensionalized interface temperature.

Figure 6(a) indicates the persistent large area contacts of ethanol. At or below this temperature the vapor film may collapse for periods of seconds while film boiling exists intermittently. Figures 6(b) and (c) reveal that at these temperatures some of the contacts may persist for more than 100 ms but eventually detaches. Additionally, there appears some large area but short time contacts as indicated by the sharp spikes on top of the long contact signals. When the interface temperature is higher than the homogeneous nucleation temperature the contact signals change. As illustrated in Figs. 6(d) and 6(e) the large area contacts detach in short time while the small area contacts persist for longer time. The small area contacts are attributed to the liquid ripples sweeping over the disk surface. This is similar to the mechanism which was observed by Moreaus et al. (13) that the liquid ripples move from the bottom to the top of a cylinder in film boiling at

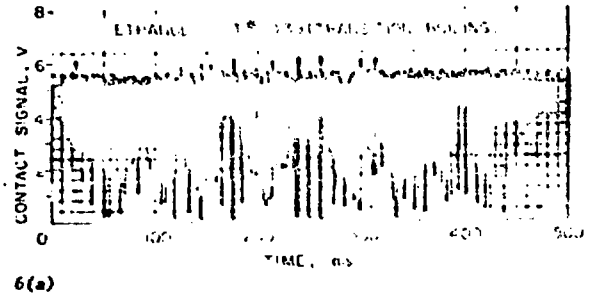

6(a)

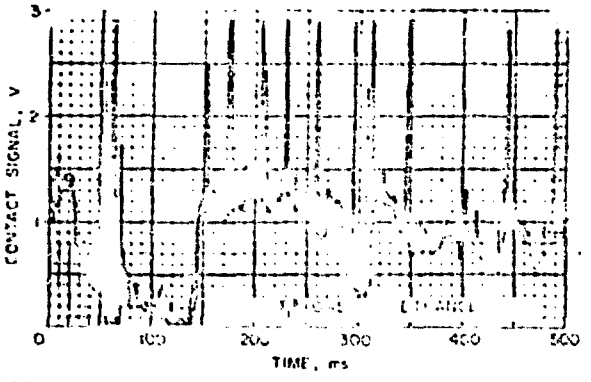

6(b)

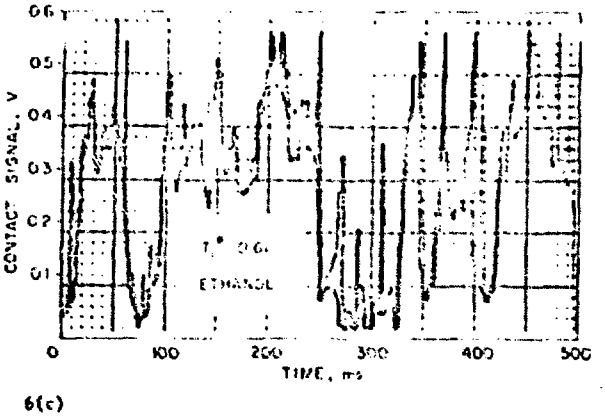

6(c)

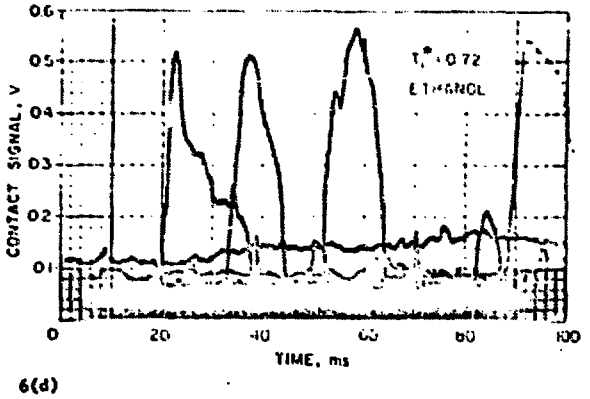

6(d)

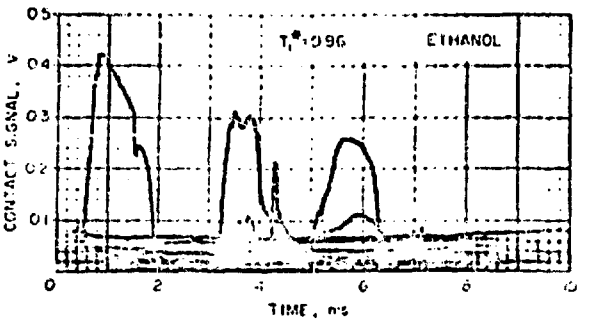

6(e)

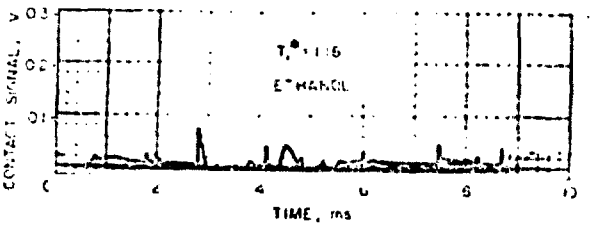

6(f)

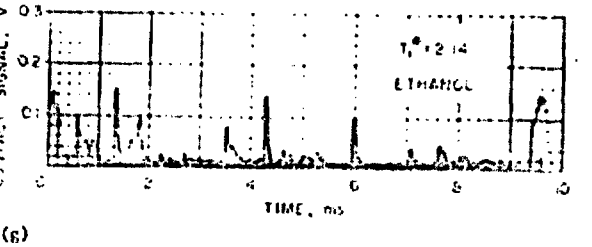

6(g)

Fig. 6(a-g). Liquid-solid contact signals of shallow ethanol to gold plated copper at different interface temperatures.

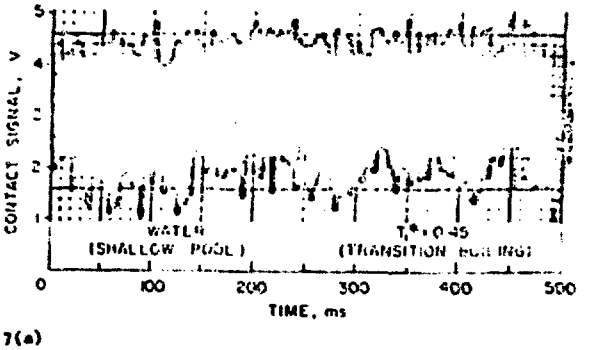

7(a)

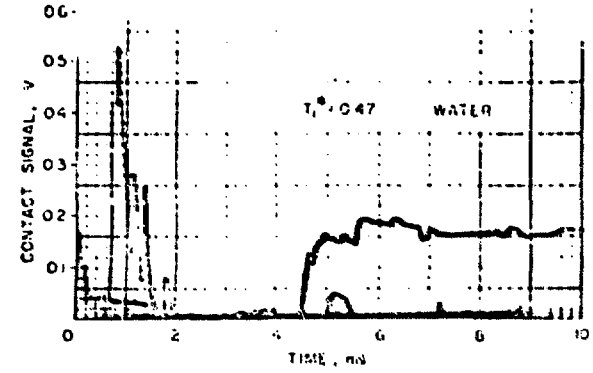

7(b)

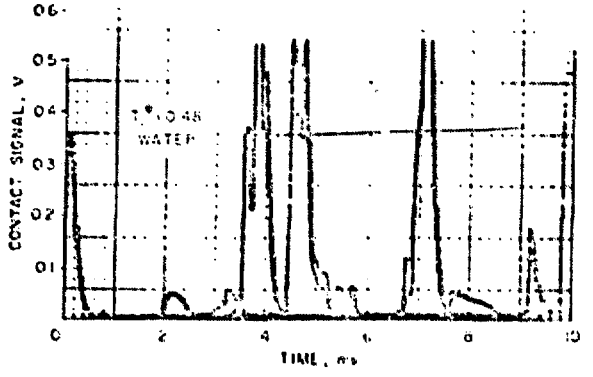

7(c)

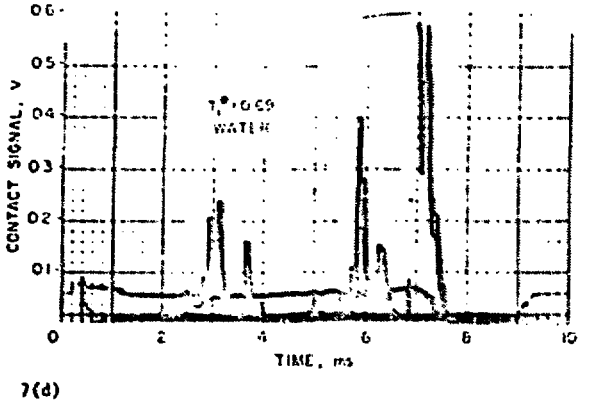

7(d)

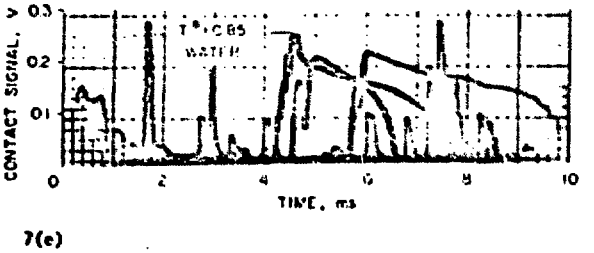

7(e)

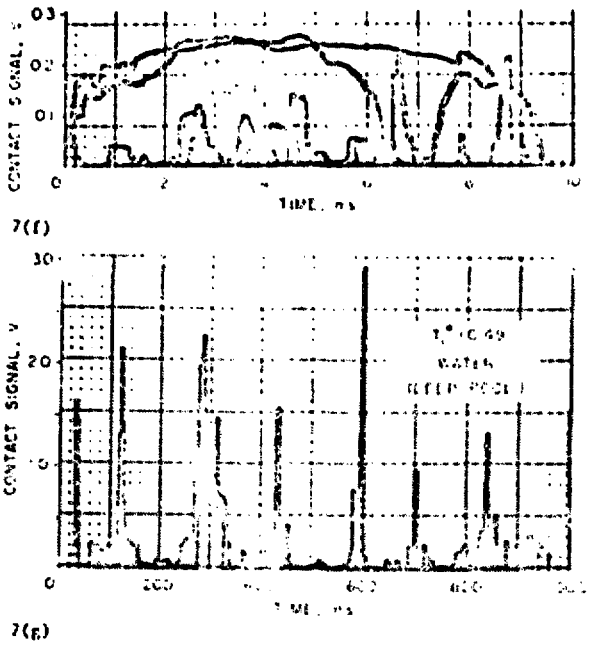

7(f)

7(g)

Fig. 7(a-g). Liquid-solid contact signals of water to gold plated copper at different interface temperatures.

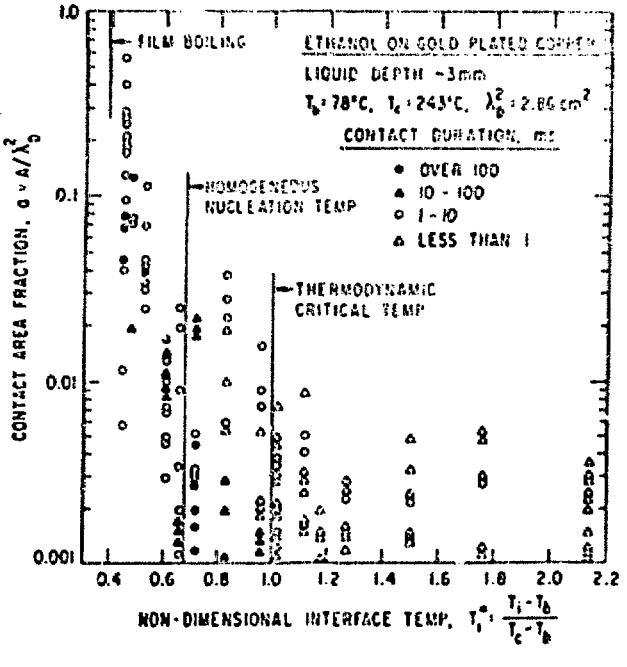

Fig. 8. The contact area fraction and the duration of contacts of ethanol at different interface temperatures.

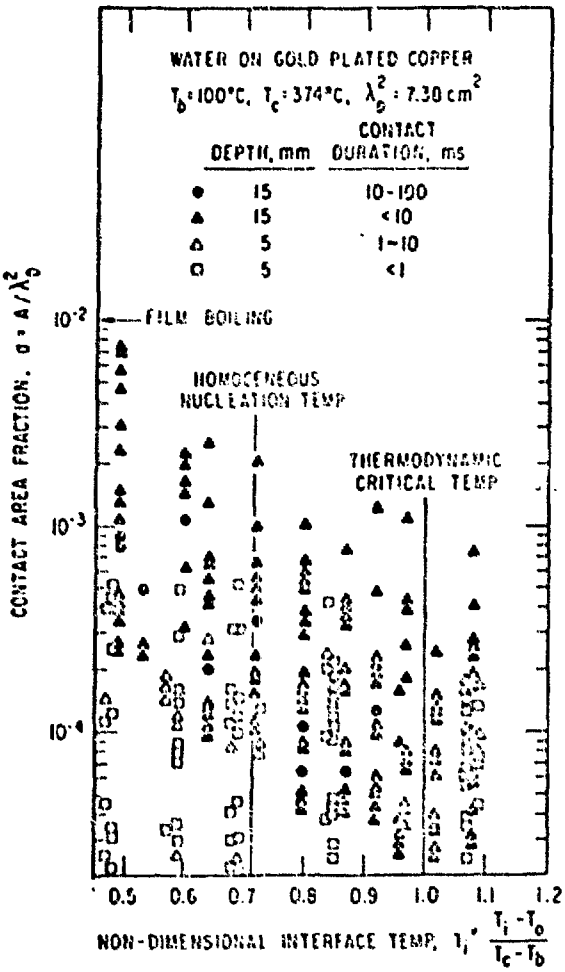

Fig. 9. The contact area fraction and the duration of contacts of water with different depth at different interface temperatures.

a velocity between 1 to 5 m/s. Figures 6(f) and 6(g) show the contact signals when the interface temperature is beyond the thermodynamic critical temperature. Most contacts are less than 1 ms and contact areas are about one order of magnitude less than that at below thermodynamic critical temperature. Figure 6 summarizes the areas and durations of contacts of ethanol. It appears that below the thermodynamic critical temperature the maximum contact area decreases exponentially as a function of nondimensional interface temperature. The duration of contact also decreases as temperature increases. Beyond the thermodynamic critical temperature the long contacts disappear and the characters of contacts are no longer a strong function of temperature.

The contact signals of water in film boiling are shown in Fig. 7. Similar to the persistent contacts in Fig. 6(a) of ethanol the persistent contact signals of water are shown in Fig. 7(a). Figures 7(b), 7(c), and 7(d) indicate that most large area contacts detach in short time while small area contacts which are induced by sweeping ripples may persist for longer time. When the interface temperature is between the homogeneous nucleation temperature and the thermodynamic critical temperature, the typical contacts are shown in Fig. 7(e). The contact durations are short. At beyond thermodynamic critical temperature most contacts are relatively smooth as indicated in Fig. 7(f). Figure 7(g) shows the contact signals of water with pool depth about 15 mm. Persistent contacts in order of 100 ms are observed. Figure 9 summarizes the water film boiling contact data. For shallow water layers the contact times are always less than 10 ms. Both the contact areas and durations are not strongly dependent on the interface temperature. For deep pool film boiling the contact areas are significantly larger than that of shallow water layer and decreases exponentially with increasing interface temperature. Long contacts, over 100 ms, are observed at deep pool only. However, at beyond thermodynamic critical temperature the long contacts disappear and the depth of liquid does not affect the contact behaviors greatly.

DISCUSSIONS OF EXPERIMENTAL RESULTS

Effects of Wetting

At the contacting process in film boiling, the vapor film between the liquid and solid has to be squeezed out. The thin vapor layer may exist originally below the liquid layer at film boiling or generated by the evaporation of the impinging liquid when it approaches the superheated vapor near the solid. Waldram et al. (14) found that when a liquid droplet impinges onto a liquid surface the intermediate vapor film will destabilize when the droplet kinetic energy per unit projection area exceeds a critical value. The vapor film stability is also shown to be a function of the surface wetting properties.

In the present experiment, before impinging to the solid the liquid has a gravitational potential energy corresponding to the height of the bubble. For case of shallow liquid layers the liquid collapses to an area equivalent to the projection area of the bubble. However, in deep pool film boiling the subsequent jet impinges the solid over a much smaller area than the bubble projection area as illustrated in Fig. 2. As a result, the impinging kinetic energy per unit area is much stronger. Therefore, larger contact area and longer contact time can be expected for deep pool film boiling due to its better chance to contact and wet the solid. The different contact behaviors of deep pool and shallow liquid layer film boiling may attribute to the different impinging mechanisms.

The transient wetting ability of the liquid to solid may also affect the liquid-solid contact and their detachment. It is observed from the steady state contact angle experiments that ethanol is a much better wetting liquid than water at room temperature. It is also known that as the liquid temperature increases the contact angle decreases and eventually equals to zero at a temperature which is between the boiling temperature and the thermodynamic critical temperature of this liquid (15). Generally ethanol has a contact angle close to zero. As a result, when the contact interface temperature is below the homogeneous nucleation temperature, the heterogeneous nucleations are not likely to happen for ethanol, and the major mechanism for liquid to detach the solid is by nucleation from preferred sites on the solid. To allow the thermal boundary layer to grow and bubbles to merge and form a vapor blanket, relatively long time is required for the

liquid to detach the solid wall. On the other hand, since water generally has a large contact angle the heterogeneous nucleation at the interface is likely to be the dominant nucleation process when the contact interface temperature is below the homogeneous nucleation temperature. The detachment of contact will be fast. In present experiments, the difference of the contact durations of shallow ethanol and water may be attributed to their different contact angles.

The Nucleation Process

As discussed previously, there are several different nucleation processes, each has different threshold temperatures, and when more than one nucleation process is possible they occur on a competitive base. The nucleation from preferred sites was described by Hsu (10) that the nucleation will not occur until the thermal boundary layer is sufficiently thick to support a critical size vapor cavity. For this kind of nucleation to occur it may take relatively long time. A similar model was proposed by Henry and Fauske (17) for the vapor explosion that the spontaneous nucleation cannot proceed until a sufficient thick thermal boundary layer has been developed to support the growth of the vapor embryon to the limit of their stability. It follows that the spontaneous nucleations occur in a short time after contact. However, if the interface temperature is higher than the thermodynamic critical temperature, the nucleation process is not restricted by surface tension any more. It is a process of property change and can occur at the interface without an appreciable time delay. The liquid-solid contact will be terminated in a short time.

It was observed from the results of ethanol and water that generally the contact duration decreases as the interface temperature increases. At beyond thermodynamic critical temperature, all the contacts are shorter than 10 ms. It appears that the duration of contacts in film boiling is dependent on the dominant nucleation process at that interface temperature. However, more definitive experiments are required to reveal the details of the nucleation and detaching processes because the measured contact duration in this experiment includes the time for bubble growth, merging, and the formation of vapor layer at the interface. Additionally, the measured total contact time is dependent on the extent of coherency of the liquid impingement.

The Contact Heat Transfer

By neglecting the microlayer evaporation contribution, the heat transfer in a liquid-solid contact can be evaluated from heat conduction consideration alone and gives a conservative estimation of contact heat transfer. Assuming the nucleation process does not affect the heat conduction in the liquid, the heat transfer can be calculated by transient heat conduction to a semi-infinite liquid region with a constant interface temperature. This gives the transient temperature profile (11)

$$T_i - T = (T_i - T_b)\,\mathrm{erf}\left(\frac{x}{2\sqrt{\alpha_l t}}\right). \tag{10}$$

The total amount of heat transferred through a contact area A in contact duration Δt is

$$Q_c = 2k_l A\sqrt{\frac{\Delta t}{\pi\alpha_l}}\,(T_i - T_b)\,. \tag{11}$$

For alternating contacts the heat flux has the form

$$q_c = 2k_l a f_c\sqrt{\frac{\Delta t}{\pi\alpha_l}}\,(T_i - T_b), \tag{12}$$

where a is the contact area fraction and f_c is the contact frequency which is 1.5 times the bubble frequency f_b. Since it was observed in Fig. 3 that the bubble frequency is linear proportional to the non-dimensional interface temperature, the bubble frequency can be presented as

$$f_b = f_{b,\min}\frac{T_i^*}{T_{i,\min}^*}\,, \tag{13}$$

where the subscript min means the value near the minimum film boiling temperature. The bubble frequency near film boiling temperature was predicted by Zuber (18) and confirmed by Hosler and Westwater (7) as

$$\frac{1}{f_{b,\min}} = 3^{0.75}\,2\pi\left[\frac{\rho_l + \rho_v}{g(\rho_l - \rho_v)}\right]^{1/2}\left[\frac{\sigma}{g(\rho_l - \rho_v)}\right]^{1/4}. \tag{14}$$

The long contacts of ethanol at below homogeneous nucleation temperature shows a contact frequency which ca not be described precisely by Eq. (2). The contact frequencies measured directly from the oscilloscope traces are used for this specific group of long contacts in the evaluation of the contact heat transfer.

Figures 10 and 11 show the contribution of liquid-solid contact heat transfer to the film boiling heat

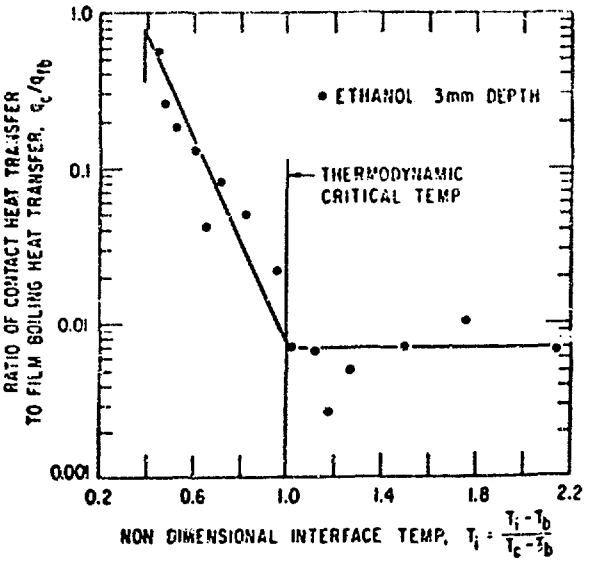

Fig. 10. Ratio of liquid-solid contact heat transfer to the film boiling heat transfer of ethanol.

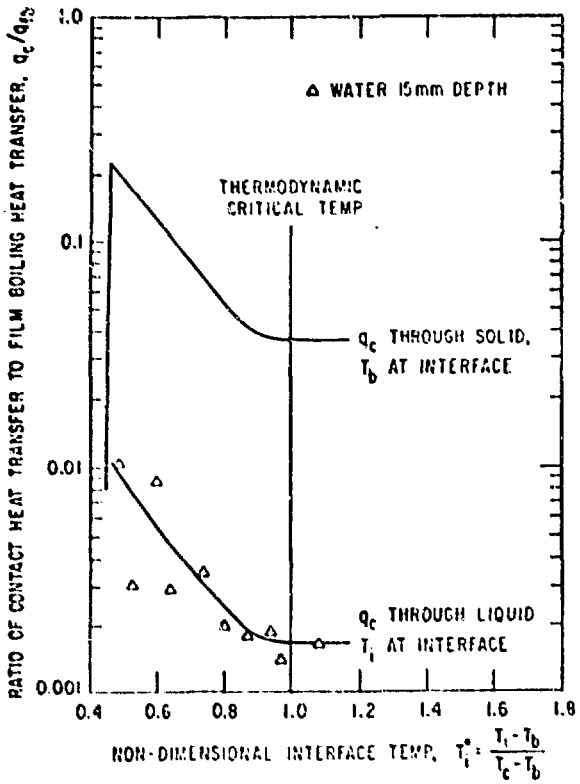

Fig. 11. Ratio of liquid-solid contact heat transfer to the film boiling heat transfer of water.

transfer at different interface temperatures. The film boiling heat fluxes are obtained from the experimental data of Hosler and Westwater (7) for water and of Bromley (19) for ethanol. Generally the contact heat transfer decreases exponentially with increasing interface temperature, then maintaining a constant level at beyond thermodynamic critical temperature. For the case of ethanol near the low temperature end of film boiling, the contact heat transfer is significant, while beyond thermodynamic critical temperature the liquid-solid contact contributes less than one percent of the overall heat transfer. The contact heat transfer of deep water pool is about one order of magnitude more than that of shallow water layer at low temperature end. As the temperature increases, the effects of liquid depth diminish.

In evaluating the heat conduction during a liquid-solid contact, another extreme condition can be considered that is to assume the vigorous nucleations occur at all the time during a contact. Under this condition, the contact interface temperature can be assumed to be at the saturation temperature of the liquid at whole contact duration. Then the heat transfer through the solid wall is in the form of

$$q_c = 2k_s a f_c \sqrt{\frac{\Delta t}{\pi a_s}} (T_s - T_b) \quad . \qquad (15)$$

Typical results of this calculation are shown in the upper curve of Fig. 10 for water. In practical circumstances the assumption of semi-infinite liquid is appropriate at the early stage of the contact duration. But the interface temperature will decrease toward the liquid saturation temperature after the nucleations occur near the interface. Since the liquid-solid contact duration of film boiling is short, the overall contact heat transfer is likely to be in between of these two estimations but closer to the lower one. For more definitive calculations, detailed knowledge of the nucleation and detaching processes are required.

In practical systems the contact heat transfer may play a very important role in film boiling when variations of the surface properties are considered. One of the examples is the film boiling on a metal surface coated with low thermal conductivity films (15, 20). Since the contact interface temperature will be lower for thicker coating, it will induce longer and larger area of liquid-solid contact. As a result, the contact heat transfer will be greatly increased and similarly the overall film boiling heat transfer. Also the transition boiling will occur at higher temperature. This phenomena was employed in the augmentation of cooling of fins operated in film boiling regime (20).

CONCLUSION

The hydrodynamic instability induced liquid-solid contacts in film boiling are observed over a wide temperature range. The area of contact is liquid depth dependent. It generally decreases exponentially with interface temperature and finally reaches a constant value at above thermodynamic critical temperature. The averaged duration of contact is influenced by the dominant nucleation process and thus dependent on the interface temperature and the wettability of the solid. The frequency of the major contacts is about 1.5 times the bubble detaching frequency.

The heat transfer due to the liquid-solid contact may account for a large percentage of the overall film boiling heat transfer near the low temperature end of film boiling and decreases exponentially as the interface temperature increases until reaching a stable value at above the thermodynamic critical temperature. The contact heat transfer in film boiling can be considered as an extension of the contact heat transfer in transition boiling. The overall film boiling heat transfer is the composition of contact heat transfer, vapor convection heat transfer, and thermal radiation, with different importance at different temperature levels.

REFERENCES

1 Bradfield, W. S., "Liquid-Solid Contact in Stable Film Boiling," I&EC Fundamentals, Vol. 5, No. 2, May 1966, pp. 200-204.

2 Bankoff, S. G., and Mahra, V. S., "A Quenching Theory for Transition Boiling," I&EC Fundamentals, Vol. 1, No. 1, Feb. 1962, pp. 38-40.

3 Henry, R. E., Quinn, D. J., and Spleha, E. A., "An Experimental Study of the Minimum Film Boiling Point for Liquid-Liquid Systems," Fifth International Heat Transfer Conf., Tokyo, Japan, Sept. 3-7, 1974.

4 Swanson, J. L., Bowman, H. F., and Smith, J. L., "Transient Surface Temperature Behavior in the Film Boiling Region," ASME Paper No. 75-HT-8.

5 Iloeje, O. E., Rohsenow, W. M., and Griffith, P., "Three-Step Model of Dispersed Flow Heat Transfer (Post CHF Vertical Flow)," ASME Paper No. 75-WA/HT-1.

6 Berenson, P. J., "Film Boiling Heat Transfer from a Horizontal Surface," J. Heat Transfer, Trans. ASME, Vol. 83, Aug. 1961, pp. 351-358.

7 Hosler, E. R., and Westwater, J. W., "Film Boiling on a Horizontal Plate," ARS Journal, April 1962, pp. 553-558.

8 Baumeister, K. J., and Hendricks, R. C., "Metastable Leidenfrost States," NASA TN D-3226, April 1966.

9 Farber, E. A., and Scorah, R. L., "Heat Transfer to Water Boiling under Pressure," Trans. ASME, May 1948, pp. 369-384.

10 Henry, R. E., "A Correlation for the Minimum Film Boiling Temperature," 14th National Heat Transfer Conf., AIChE Preprint 14, 1973.

11 Carslaw, H., and Jaeger, J., Conduction of Heat in Solids, 2nd ed., Oxford, Clarendon Press, 1959.

12 Cole, R., "Boiling Nucleation," Advance in Heat Transfer, Vol. 10, pp. 85-166.

13 Moreau, P., Chevrier, J. C., and Beck, G., "Destabilization of Film Boiling by Means of a Thermal Resistance," Int. J. Multiphase Flow, Vol. 2, 1975, pp. 183-190.

14 Waldram, K. L., Fauske, H. K., and Bankoff, S. G., "Impaction of Volatile Liquid Droplets onto a Hot Liquid Surface," ASME Paper No. 75-HT-10.

15 Adamson, A. W., "Potential Distortion Model for Contact Angle and Spreading, II. Temperature Dependent Effects," J. Colloid and Interface Sc., Vol. 44, No. 2, Aug. 1973, pp. 273-281.

16 Hsu, Y. Y., and Graham, R. W., NASA Report TN-D-595, 1961.

17 Henry, R. E., and Fauske, H. K., "Energetics of Vapor Explosions," ASME Paper No. 75-HT-66.

18 Zuber, N., and Tribus, M., "Further Remarks on the Stability of Boiling Heat Transfer," Report 58-5, University of California, Los Angeles, 1958, p. 40.

19 Bromley, L. A., "Heat Transfer in Stable Film Boiling," Ch. Eng. Progress, Vol. 46, No. 5, 1950, pp. 221-227.

20 Zhukov, V. M., et al., "Heat Transfer in Boiling of Liquids on Surfaces Coated with Low Thermal Conductivity Films," Heat Transfer-Soviet Research, Vol. 7, No. 3, 1975, pp. 16-26.